

## Searching for Rate Determining Step of CNT Formation: The Role of Cementite

Lorenzo Pellegrino\*, Matteo Daghetta, Renato Pelosato, Attilio Citterio, Carlo V. Mazzocchia

Dipartimento di Chimica, Materiali e Ingegneria Chimica "Giulio Natta" Politecnico di Milano, Piazza Leonardo da Vinci 32, Milano, Italy  
[lorenzo.pellegrino@chem.polimi.it](mailto:lorenzo.pellegrino@chem.polimi.it)

We produce multiwall carbon nanotubes in a large-scale fluidized bed reactor, in which catalytic chemical vapour deposition occurs. The catalyst employed is iron supported over alumina, whereas the carbon source is ethylene, which is fed together with hydrogen and nitrogen.

In order to reach a deep knowledge of the mechanism and parameters involved in the growth of carbon nanotubes, the role of different conditions and variables has been investigated: the preparation method of the catalyst, the iron percentage, ethylene and hydrogen partial pressures in the gas feed. One of the reactions that takes place during the whole process, is  $\text{Fe}_3\text{C}$  (cementite) formation. The role of iron carbide has been considered by many authors, although they are not completely in agreement about it. The phase evolution of the system has been investigated via X-Ray Powder Diffraction (XRPD) at different reaction times. On the basis of our experimental data, we suggest that iron carbide is an intermediate which is formed in the early stages of the reaction and subsequently decomposes to form CNTs.

### 1. Introduction

Carbon nanotubes, either singlewall (SWCNT) or multiwall (MWCNT), are finding various applications in many fields. Their use will be as more extensive as their production costs will drop (mainly depending on the market demand) and some technical problems will be solved (i.e. their uniform dispersion in a matrix). Applications comprise electronic devices, nanocomposites and coatings (Wernik et al., 2010), gas separation and sensors (Ampelli et al. 2012), drug delivering (Vashist et al., 2011) and others. In the past four years a viable way for synthesis of multiwall carbon nanotubes (MWCNTs) has been studied and developed by our group (Mazzocchia et al., 2009). It is based on a large scale fluidized bed reactor in which a catalytic chemical vapour deposition (FBCCVD) occurs. In suitable conditions, 400 g/batch of MWCNTs can be prepared. An iron based catalyst, supported over alumina, is used, while ethylene is the carbon source.

In order to reach a good knowledge of the mechanism and parameters involved in the growth of carbon nanotubes, the role of different variables has been investigated, like as the preparation method of the catalyst, the iron percentage, ethylene and hydrogen partial pressures in the gas feed.

Recently the attention has been focused on cementite ( $\text{Fe}_3\text{C}$ ), whose role has been considered by different authors (Philippe et al., 2009), although they are not completely in agreement about it (Coquay et al., 2002).

### 2. Experimental

The catalyst has been prepared by wet impregnation starting from  $\gamma$ -alumina and a suitable Fe(III) salt dissolved in methanol, following the method described by Mazzocchia et al. (2010). The resulting solid has been calcined in air at 500 °C, yielding to hematite over alumina material. The iron content was 18.7 % wt. respect to alumina, as measured by ICP analysis. The catalyst has been then conditioned under nitrogen at 600 °C and then reduced at the same temperature with hydrogen by using a quartz cylindrical reactor

equipped with a gas distributor in fluidized bed reactor regime. This reactor, 3.2 cm in diameter and 100 cm in height, is a *scale down* of a larger reactor which works with the same principle.

The gas flow has been fixed at  $5.5 \cdot 10^{-5} \text{ Nm}^3/\text{s}$  and the composition was 30 % vv. hydrogen and 70 % vv. nitrogen during the reduction step and 30 % vv. hydrogen, 20 % vv. ethylene, 50 % vv. nitrogen during the CNT production step (Mazzocchia et al., 2009).

The outlet gas stream composition has been continuously monitored through an Agilent micro-GC.

Different samples have been collected during the two reaction steps using standard Schlenk technique.

X-ray powder diffraction data (XRPD) have been collected at room temperature with a Bruker D8 diffractometer, using graphite monochromated Cu-K $\alpha$  radiation. The step scan was  $0.02^\circ 2\theta$  and the measurement time 12 s/step. The samples have been ground in an agate mortar. The phase analysis has been performed by using the DiffracPlus Evaluation software (Bruker AXS).

Pristine carbon nanotubes were characterized by Scanning Electron Microscopy (SEM, ZEISS EVO<sup>®</sup> 50 EP) and High Resolution Transmission Electron Microscopy (HRTEM, JEOL, JEM-2100 LaB<sub>6</sub>). In the latter case a sample of CNTs was dispersed in water by sonication and put on a copper grid covered with 300 mesh Holey Carbon.

### 3. Results

The hematite phase, present in the catalyst, has been reduced in a N<sub>2</sub>/H<sub>2</sub> stream at 600 °C for 2700 s, then the system has been cooled down to RT for XRPD sampling. The following procedure, repeated three times, has been applied for reaction monitoring of CNT synthesis:

- Heating of the catalyst up to 600 °C in N<sub>2</sub> stream (1800 s);
- Reaction at 600 °C in N<sub>2</sub>/H<sub>2</sub>/C<sub>2</sub>H<sub>4</sub> stream (900 s);
- Cooling down at RT in N<sub>2</sub> stream (2700 s);
- Sampling under N<sub>2</sub> atmosphere.

Three samples, have been taken after 900 s, 1800 s and 2700 s. XRPD patterns have been collected for all samples and normalized with respect to the  $\gamma\text{-Al}_2\text{O}_3$  peak at about  $67^\circ 2\theta$  (Figure 1).

After 2700 s of reduction, no hematite is present, only a small residue of magnetite remains and iron is the main species, as shown in figure 1a.

After the first reaction step, iron peaks are still present and cementite peaks are also clearly evident (Figure 1b).

Moreover, graphitized carbon peaks confirm the formation of carbon nanotubes.

Both iron and cementite reduce their peak intensities after 1800 s (Figure 1c) and finally, after the third reaction step, cementite is no longer present and only graphitic carbon is evident (Figure 1d).

Table 1 summarizes the identified phases and their respective database patterns.

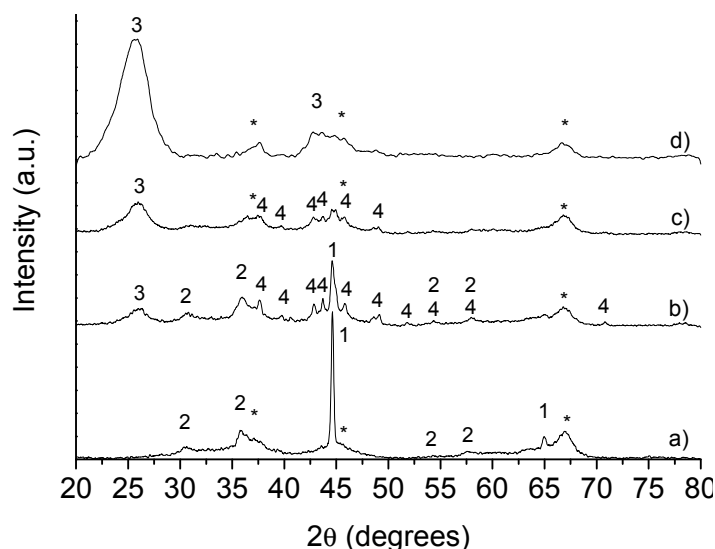


Figure 1: XRPD pattern of a) catalyst after 2700 s of reduction; b) sample after 900 s reaction; c) sample after 1800 s reaction; d) sample after 2700 s reaction.

Table 1: XRPD spectra legend

Label	Species	ICDD-PDF Database
*	$\gamma\text{-Al}_2\text{O}_3$	(PDF # 00-10-0425)
1	Fe	(PDF # 00-06-0696)
2	$\text{Fe}_3\text{O}_4$	(PDF # 01-75-0449)
3	C graphite	(PDF # 01-75-1621)
4	$\text{Fe}_3\text{C}$	(PDF # 00-35-0772)

Scanning electron microscopy (SEM) confirmed the formation of carbon nanotubes (Figure 2 left) and the presence of the catalyst inside the CNT entanglements is evidenced also by EDX analysis (Figure 2 right).

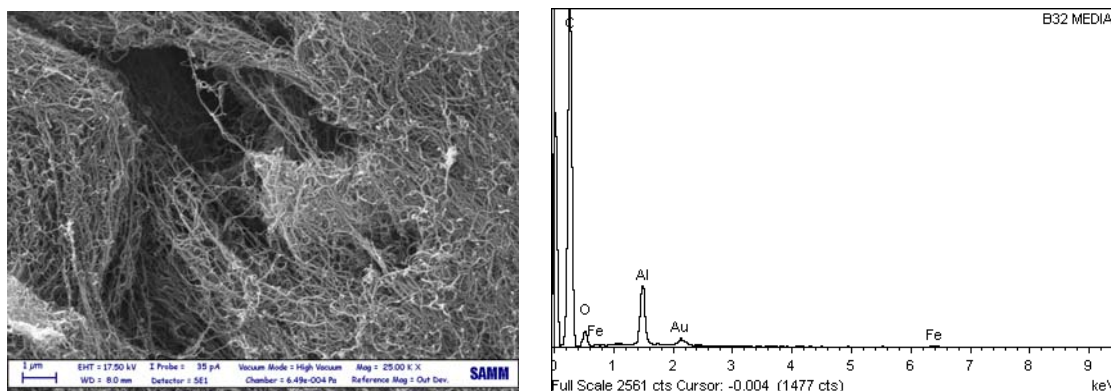


Figure 2: left) SEM image of pristine MWCNTs after 2700 s of reaction right) average EDX analysis

TEM images highlight the presence of metallic nanoparticles inside the nanotubes (Figure 3 right), revealing that the tip growth mechanism is acting in this case. Catalyst is also evident outside the nanotubes (Figure 3 left).

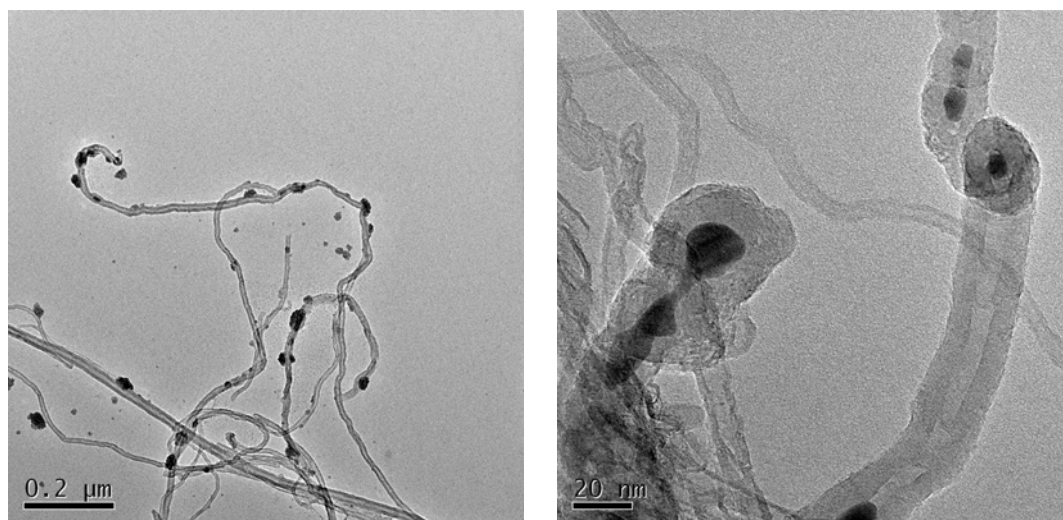


Figure 3: TEM image of pristine MWCNTs after 2700 s of reaction. Left) metallic nanoparticles are present outside the nanotubes (black particles) Right) ferrous nanoparticles (dark spots) are allocated in the tip of carbon nanotubes.

#### 4. Discussion

Different authors have focused their attention on the role of  $\text{Fe}_3\text{C}$  in the formation of carbon nanotubes, which has been considered as an active catalytic phase ( Wirth et al., 2012), an intermediate for graphitic structure formation ( Zaikovskij et al., 2001) or even a starting point for graphene production (Su et al., 2012). Most of them use an *in-situ* analytical approach, like environmental transmission electron microscopy, which can not leave fixed bed and microreactor systems aside. Such approach was

unsuitable for us. In fact, being interested in the optimization of a FBCCVD, we wanted to be as close as possible to our production scale reactor, as the catalyst behaviour in a fixed bed reactor can be completely different from a fluidized bed one. The knowledge of the real growth mechanism of carbon nanotubes is fundamental in order to find the rate determining step of the whole synthesis and so to accelerate the reaction and to optimize the production. So a simplified reaction scheme has to be applied. Gas chromatography revealed the presence of unreacted ethylene, ethane and methane in traces. GC data, coupled with XRPD spectra, can be justified by assuming the occurrence of the following reactions:

- 1) Ethylene cracking:  

$$\text{C}_2\text{H}_4 \longrightarrow 2\text{C}_{\text{amorph.}} + 2\text{H}_2 \quad K(873 \text{ K}) = 2.64 \cdot 10^8$$
- 2) Iron carbide formation:  

$$3\text{Fe} + \text{C}_{\text{amorph.}} \longrightarrow \text{Fe}_3\text{C} \quad K(873 \text{ K}) = 5.50 \cdot 10^{-1}$$
- 3) Iron carbide decomposition – graphitization:  

$$\text{Fe}_3\text{C} \longrightarrow \text{C}_{\text{graph.}} + \text{Fe} \quad K(873 \text{ K}) = 1.81$$
- 4) Ethylene hydrogenation:  

$$\text{C}_2\text{H}_4 + \text{H}_2 \longrightarrow \text{C}_2\text{H}_6 \quad K(873 \text{ K}) = 3.25$$
- 5) Methane formation from carbon:  

$$\text{C} + 2\text{H}_2 \longrightarrow \text{CH}_4 \quad K(873 \text{ K}) = 5.30 \cdot 10^{-3}$$
- 6) Methane production from ethylene  

$$\text{C}_2\text{H}_4 + 2\text{H}_2 \longrightarrow 2\text{CH}_4 \quad K(873 \text{ K}) = 9.55 \cdot 10^1$$

Reactions 1-3 are undoubtedly the main reaction which yields to carbon nanotubes, while reactions 4-6 are parasite reactions. Their products, ethane and methane are usually detected in low concentration in the outlet gas stream. Reaction 3 equilibrium constant is evaluated according to Ci et al. (2001), who computed the Gibbs free energy of graphitization of carbon nanotubes. About the role of cementite in the nanotube formation process, it should have a key role, even if there is not a complete agreement among authors.

For example, He et al. (2011) claimed that carbon nanofibers, which are closely related to CNTs, can be formed both via  $\text{Fe}_3\text{C}$  and directly from  $\alpha\text{-Fe}$ . These species should have a catalytic role, and they are found in the tip of CNFs at the end of the reaction. Authors performed growth experiments at 600, 650 and 725 °C, finding only  $\text{Fe}_3\text{C}$  at 600 °C and both  $\text{Fe}_3\text{C}$  and  $\alpha\text{-Fe}$  at higher temperature. They conclude that, at 600 °C, all the iron is converted to cementite, which is the only catalytically active species. Likewise Yoshida et al. (2008) found only cementite at 600°C. On the contrary, in our case iron is clearly present at 600 °C, together with cementite, even if XRPD peaks decrease in intensity during the reaction proceeding. Also Sharma et al. (2009) and Wirth et al. (2012) consider  $\text{Fe}_3\text{C}$  as a catalyst at 600 °C.

On the other hand, Schaper et al. (2004) proved that carbon nanotubes are produced via the formation of an intermediate iron carbide ( $\text{Fe}_3\text{C}$ ) phase. Moreover, Ni et al. (2009) found that CNTs form from the decomposition of metal carbides ( $\text{Fe}_3\text{C}$ ,  $\text{Co}_2\text{C}$ ,  $\text{Ni}_3\text{C}$ ), while Zaiakovskij et al. (2002) concluded that the formation of carbon nanotubes is explainable in terms of a carbide cycle mechanism. Finally Su et al. (2012) found that, in particular conditions,  $\text{Fe}_3\text{C}$  inside the CNT can decompose to give graphene.

A possible explanation of such different results can arise from the consideration that the growth of graphitic material is particularly boundary condition sensitive and not always the various experimental conditions used by authors are exactly comparable, leading to conclusions which are true in the examined case, but they might lack for a universality peculiarity.

Ferrite ( $\alpha\text{-iron}$ ) has a bcc crystal lattice, whose interstitial position configuration and dimension do not allow easy accommodation of C atoms. For this reason, carbon solubility in ferrite does not achieve high values, being below 0.1 at % in  $\alpha\text{-Fe}$  (Hasebe et al., 1985).

As evidenced by Fe-C diagram state, cementite is a metastable compound, whose formation occurs when solubility limit exceeds 0.055% molar ratio. Yet metallurgical data show that cementite formation times are very long, but, when small iron particles are present (50-200 nm), the reaction proceeds faster (Callister, 2007). Bulk  $\text{Fe}_3\text{C}$  melting point is about 300 °C below bulk Fe melting point and the same trend should be shown by carbide and pure metal nanoparticles, which melt at temperatures decreasing with their sizes (Benissad et al., 1988 and Ding et al., 2004).

For these reasons, carbon solubility in iron carbide is higher than in pure iron (Sharma et al., 2009).

Cementite decomposition is almost thermodynamically favorable, as outlined by reaction 3 equilibrium constant. This is confirmed by our experimental results, as shown by XRPD spectrum in figure 1, and by the results of Zhang et al. (2001) which found  $\text{Fe}_3\text{C}$  to be unstable at 600 °C.

Spectra of samples withdrawn at different reaction times (figure 1 b-d), show that cementite percent amount decreases over time until its disappearance. Particularly figure 1b shows that, in the early stages

of the synthesis, several species are present, emphasizing a transitory situation. So, arising from this facts, it is quite clear that reactions 1-6 occur at the same time and iron is not completely converted to cementite before CNT formation starts. On the basis of our XRPD results, it can be confirmed that cementite formation is a necessary step in MWCNT synthesis, as no nanotubes growth was observed using metals that do not yield to carbides (Esconlauregui et al., 2009). Then carbon nanotubes grow up from carbide decomposition and probably in this step amorphous carbon, arising out of ethylene cracking (reaction 1), moves to graphitic one.

Iron peaks in the pattern of the sample withdrawn at the end of the reaction (figure 1d) are not easily revealed because catalyst milling, induced by MWCNT growth, reduces crystallite size and so their X-ray diffraction capability. Moreover spectrum 1d has the highest graphite peaks, and iron fluorescence during XRPD data collection could mask the reflections of the phases containing iron, especially when iron and iron carbide amounts decrease with time (figure 1). TG analysis (figure 4) of the sample withdrawn after 2700 s, shows that a residue is present after oxidation up to 900 °C, that is the catalyst used for MWCNT synthesis. So it is possible to conclude that iron is still present, but it evolves to a not-crystalline phase and even if a small quantity of thin crystalline iron particles remains in the system, it is not easily detectable by XRPD.

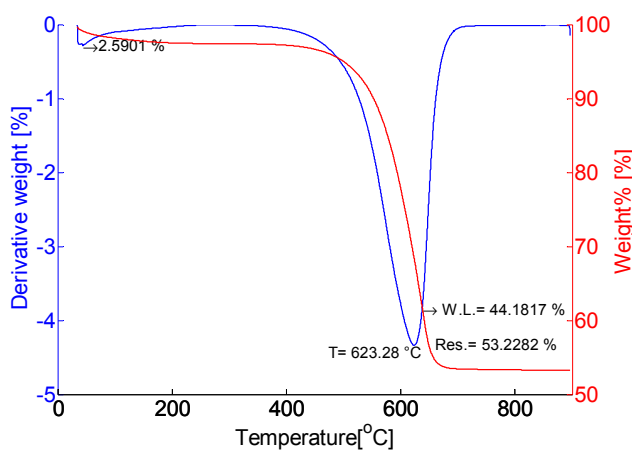


Figure 4: Thermogravimetric analysis of the sample withdrawn at 2700 s.

Our experimental data indicate that reactions 2 and 3 could be designed as candidates for rate determining step (RDS) of CNT synthesis. We are currently collecting more data and proceeding to other characterization, as well as testing other process conditions, in order to achieve the objective of finding the RDS.

## 5. Conclusions

XRPD demonstrated that, at 600 °C, iron is gradually converted into cementite in a  $N_2/C_2H_4/H_2$  atmosphere, while carbon nanotubes are formed, most likely from the decomposition of the latter. In fact,  $Fe_3C$  is known to be unstable at 600 °C and peak intensities of both the species decrease during the reaction until, after 2700 s, they are negligible. As expected working at relatively low temperature, iron nanoparticles are not able to evaporate from the reaction ambient, as reported by Su et al. (2012) which work at 1000 °C. So Fe is still present in the nanotubes at the end of the reaction, as confirmed by ICP, EDX, SEM and TEM analyses.

## Acknowledgements

Authors are grateful to Ministero dell'Istruzione, Università e Ricerca for funding this research (PRIN 2009). SMM laboratory (Dario Picononi) and Università degli Studi di Palermo (Prof. Eugenio Caponetti) are acknowledged for SEM and TEM images respectively. Authors thank Dr. Monica Dapiaggi and Dr. Nicoletta Marinoni (Università degli Studi di Milano) for the help in data interpretation.

## References

- Ampelli C., Spadaro D., Neri G., Donato N., Latino M., Passalacqua R., Perathoner S., Centi G., 2012, Development of hydrogen leak sensors for fuel cell transportation, *Chemical Engineering Transaction*, 26, 333-338, DOI: 10.3303/CET1226065
- Benissad, F., Gadelle, P., Coulon, M., Bonnetain, L., 1988, Carbon fibre formation from methane, part II: carbon germination and catalyst particles fusion (*Formation de fibres de carbone a partir du methane II: Germination du carbone et fusion des particules catalytiques.*), *Carbon* 26, 425-432, DOI: 10.1016/0008-6223(88)90141-8.
- Callister W.D., 2007, *Materials science and engineering: an introduction* 721 pp. John Wiley & Sons, United States of America. ISBN: 9780470120323.
- Ci L., Wei B., Xu C., Liang J., Wu D., Xie S., Zhou W., Li Y., Liu Z., Tang D., 2001, Crystallization behavior of the amorphous carbon nanotubes prepared by the CVD method. *Journal of Crystal Growth* 233, 823-828., DOI: 10.1016/S0022-0248(01)01606-2
- Coquay P., Peigney A., De Grave E., Vandenberghe R.E., Laurent C., 2002, Carbon Nanotubes by a CVD Method. Part II: Formation of Nanotubes from (Mg, Fe)O Catalysts., *J. Phys. Chem. B.* 106(51):13199-13210, DOI: 10.1021/jp026632k.
- Ding, F., Bolton, K., Rosen, A., 2004, Iron-carbide cluster thermal dynamics for catalyzed carbon nanotube growth. *Journal of Vacuum Science & Technology A: Vacuum, Surfaces, and Films* 22, 1471-1476, DOI: 10.1116/1.1752895
- Esconlauregui S., Whelan C. M., Maex K., 2009, The reasons why metals catalyse the nucleation and growth of carbon nanotubes and other carbon nanomorphologies. *Carbon*. 47, 659-669, DOI: 10.1016/j.carbon.2008.10.047.
- Fam D.W.H., Palaniappan A., Tok A.I.Y., Liedberg B., Moochhala S.M., 2011, A review on technological aspects influencing commercialization of carbon nanotube sensors. *Sensors and Actuators B: Chemical*. 157(1):1-7, DOI: 10.1016/j.snb.2011.03.040.
- Hasebe, M., Ohtani, H., Nishizawa, T., 1985, Effect of magnetic transition on solubility of carbon in bcc Fe and fee Co-Ni alloys. *Metall. Mater. Trans.* 16, 913-921.
- He Z., Maurice, J.-L., Gohier, A., Lee, C.S., Pribat, D., Cojocar, C.S., 2011, Iron Catalysts for the Growth of Carbon Nanofibers: Fe, Fe<sub>3</sub>C or Both? *Chem. Mater.* 23, 5379-5387, DOI: 10.1021/cm202315j.
- Ni, L., Kuroda, K., Zhou, L.-P., Ohta, K., Matsuishi, K., Nakamura, J., 2009. Decomposition of metal carbides as an elementary step of carbon nanotube synthesis. *Carbon* 47, 3054-3062, DOI:10.1016/j.carbon.2009.07.009.
- Mazzocchia C., Nunga P., Tito A., Bestetti M., Bianco F., 2009, article n° 617, XII<sup>eme</sup> Congrès de la Société Française de Génie des Procédés, Marseille, France.
- Mazzocchia C., Bestetti M., Acierno D., Tito A., 2010, A process for the preparation of a catalyst, a catalyst obtained thereby, and its use in the production of nanotubes. *Eur. Patent* 2213369 (A1).
- Philippe R., Caussat B., Falqui A., Kihn Y., Kalck, P., Bordère S., Plee D., Gaillard P., Bernard D., Serp P., 2009. An original growth mode of MWCNTs on alumina supported iron catalysts. *Journal of Catalysis* 263, 345-358., DOI: 10.1016/j.jcat.2009.02.027
- Schaper A.K., Hou H., Greiner A., Phillipp F., 2004, The role of iron carbide in multiwalled carbon nanotube growth. *Journal of Catalysis* 222(1):250-254, DOI: 10.1016/j.jcat.2003.11.011.
- Sharma R., Moore E., Rez P., Treacy M.M.J., 2009, Site-Specific Fabrication of Fe Particles for Carbon Nanotube Growth. *Nano Letters*, 9(2):689-694, DOI: 10.1021/nl803180e.
- Su, Q., Li, J., Du, G., Xu, B., 2012, In Situ TEM Study on the Electrical and Field-Emission Properties of Individual Fe<sub>3</sub>C-Filled Carbon Nanotubes. *J. Phys. Chem. C* 116, 23175-23179.
- Vashist S.K., Zheng D., Pastorin G., Al-Rubeaan K., Luong J.H.T., Sheu F.S., 2011, Delivery of drugs and biomolecules using carbon nanotubes. *Carbon*. 49(13):4077-97, DOI: 10.1016/j.carbon.2011.05.049.
- Wernik J.M., Meguid S.A., 2010, Recent Developments in Multifunctional Nanocomposites Using Carbon Nanotubes. *Applied Mechanics Reviews*.63(5):050801, DOI: 10.1115/1.4003503.
- Wirth, C.T., Bayer, B.C., Gamalski, A.D., Esconjauregui, S., Weatherup, R.S., Ducati, C., Baehtz, C., Robertson, J., Hofmann, S., 2012, The Phase of Iron Catalyst Nanoparticles during Carbon Nanotube Growth. *Chem. Mater.* 24, 4633-4640, DOI: 10.1021/cm301402g.
- Yoshida, H., Takeda, S., Uchiyama, T., Kohno, H., Homma, Y., 2008, Atomic-Scale In-situ Observation of Carbon Nanotube Growth from Solid State Iron Carbide Nanoparticles. *Nano Lett.* 8, 2082-2086, DOI: 10.1021/nl080452q.
- Zaikovskij, V.I., Chesnokov, V.V., Buyanov, R.A., 2002, Formation of Carbon Filaments from 1,3-Butadiene on Fe/Al<sub>2</sub>O<sub>3</sub> Catalysts. *Kinetics and Catalysis* 43, 677-683, DOI: 10.1023/A:1020604129725.
- Zhang, J., Ostrovski, O., 2001, Cementite Formation in CH<sub>4</sub>-H<sub>2</sub>-Ar Gas Mixture and Cementite Stability. *ISIJ International* 41, 333-339.